Finite-Element Analysis of Quantum Wells of Arbitrary Semiconductors with Arbitrary Potential Profiles

KENJI NAKAMURA, AKIRA SHIMIZU, MASANORI KOSHIBA, SENIOR MEMBER, IEEE, AND KAZUYA HAYATA

Abstract—**A finite-element method for the analysis of eigenstates in a quantum well, which is made of arbitrary semiconductors and which has arbitrary potential profile, is developed. The method is based on the Galerkin procedure, and third-order Hermitian line elements are used for finite elements. A general boundary condition of the envelope function at the heterointerface is introduced by using the transfer matrix. The validity of the method is confirmed by calculating the eigenstates of GaAs/AlGaAs and InAs/GaSb rectangular quantum wells. Numerical examples of voltage-applied quantum wells are also presented.**

I. Introduction

With the recent improvement in epitaxial crystal growth techniques such as MBE and MOCVD, it has become possible to fabricate high-quality layered semiconductor structures like quantum wells (QW's) and potential barriers. These structures have been attracting much attention in these years because of their electronic [1], [2] and optoelectronic [3], [4] properties. In the design of QW devices, it is important to know the eigenstates (eigenenergies and eigenfunctions) of QW's. Within the effective mass approximation, this reduces to solving the Schrödinger equation for the envelope function.

When the potential is constant or linear in the region, the Schrödinger equation can be solved exactly [5]–[7]. However, when we consider an arbitrary potential profile, the Schrödinger equation must be solved by a numerical method. Numerical methods based on the multistep potential approximation [8], [9], piecewise-linear potential approximation [10]–[12], and transmission line analogy [13] have been successfully developed for the analysis of QW's with arbitrary potential profiles. On the other hand, finite-element methods are developed by Miyoshi *et al.* [14] and the authors [15]. The method by Miyoshi *et al.* is based on a functional, and thus is difficult to extend to dissipative and/or nonlinear systems. By contrast, the method by the authors is more extensible because it is based on the Galerkin method [16].

When we solve the Schrödinger equation for the envelope function, we have to be careful about the boundary condition at heterointerfaces. In a GaAs/AlGaAs system, the boundary condition has the well-known form that the envelope function, and its derivative divided by effective mass, are continuous at the interfaces. As yet, the numerical analyses of QW's and potential barriers are based on this boundary condition. However, in the systems made of other materials such as InAs/GaSb, this boundary condition is not appropriate. For a general boundary condition of the envelope function at the heterointerface, Ando *et al.* proposed a *transfer matrix* which gives a linear relation between the envelope function and its first derivative at the interface [17], [18].

In this paper, a finite-element method using the transfer matrix of the heterointerface is described, which is valid for a QW of arbitrary semiconductors with arbitrary potential profile. The method is based on the Galerkin procedure. The general boundary condition using the transfer matrix is incorporated by using third-order Hermitian line elements [16] for finite elements. Numerical examples on rectangular QW's of GaAs/AlGaAs (where the envelope function, and its first derivative divided by effective mass, are continuous at the heterointerfaces) and InAs/GaSb (where they are discontinuous) are given. We also apply our method to the QW subject to an external electric field.

II. Basic Equation

We consider a QW with arbitrary potential profile as shown in Fig. 1. Within the effective mass approximation, the envelope function Ψ of a particle, an electron or a hole, in the QW is given by the one-dimensional time-independent Schrödinger equation

$$\left(-\frac{\hbar^2}{2}\frac{d}{dz}\frac{1}{m_e(z)}\frac{d}{dz}+U(z)\right)\Psi(z)=E\Psi(z) \quad (1)$$

where $2\pi\hbar$ is Planck's constant, $m_e(z)$ is the effective mass of the particle, $U(z)$ is the potential, and E is the energy of the particle. In order to reduce the number of parameters, the coordinate z, the potential $U(z)$, and the energy E are normalized as $\zeta = z/d$, $u(\zeta) = U(z)/E_1$, and $\epsilon = E/E_1$, respectively, where $E_1 = \hbar^2\pi^2/2m_e(0)\,d^2$ is the eigenenergy of the ground state in a rectangular QW with the well width d and the infinite well depth, and $m_e(0)$ is the effective mass of the particle at $z = 0$. With

Manuscript received September 9, 1988; revised December 17, 1988.

K. Nakamura and A. Shimizu are with the Research Center, Canon Inc., 5-1 Morinosato-Wakamiya, Atsugi, Kanagawa, 243-01 Japan.

M. Koshiba and K. Hayata are with the Department of Electronic Engineering, Hokkaido University, Kita 13, Nishi 8, Kitaku, Sapporo, 060 Japan.

IEEE Log Number 8926835.

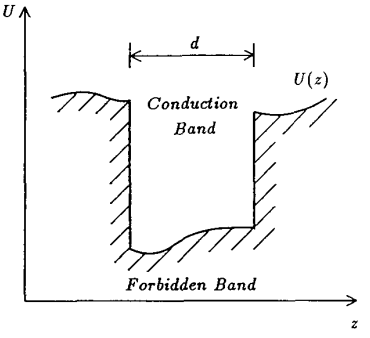

Fig. 1. Quantum well with arbitrary potential profile.

this notation, the Schrödinger equation (1) is reduced to

$$\left(-\frac{1}{\pi^2}\frac{d}{d\zeta}\frac{1}{m^*(\zeta)}\frac{d}{d\zeta}+u(\zeta)\right)\Psi(\zeta)=\epsilon\Psi(\zeta) \quad (2)$$

where $m^*(\zeta)=m_e(z)/m_e(0)$.

III. Method of Analysis

A. Finite-Element Method

In the present analysis, we consider a particle bound in the QW. Then the envelope function Ψ satisfies

$$\Psi(\zeta)\rightarrow 0(\zeta\rightarrow\pm\infty). \quad (3)$$

Thus, instead of treating the infinite region $-\infty\le\zeta\le\infty$, we can use the approximation that the envelope function $\Psi(\zeta)$ is zero out of the region $\zeta_l\le\zeta\le\zeta_r$, and that the boundary condition is given by

$$\Psi(\zeta_l)=\Psi(\zeta_r)=0 \quad (4)$$

where $\zeta_l\le\zeta\le\zeta_r$ is a sufficiently wide region that includes the QW.

Dividing the region $\zeta_l\le\zeta\le\zeta_r$ into a number of third-order Hermitian line elements [16] of Fig. 2, Ψ within each element are defined in terms of the value of envelope function Ψ_k and its derivative $\Psi_k'(=(d\Psi/d\zeta)|_{\zeta=\zeta_k})$ at the nodal point k on $\zeta=\zeta_k(k=1,2)$ as follows:

$$\Psi=\{N\}^T\{\Psi\}_e \quad (5)$$

where

$$\{\Psi\}_e=[\Psi_1\quad\Psi_2\quad\Psi_1'\quad\Psi_2']^T \quad (6)$$

$$\{N\}=[N_1\quad N_2\quad N_3\quad N_4]^T. \quad (7)$$

Here T, $\{\cdot\}$, and $\{\cdot\}^T$ denote a transpose, a column vector, and a row vector, respectively, and the shape functions N_1–N_4 are given by

$$N_1=2s^3-3s^2+1 \quad (8)$$

$$N_2=-2s^3+3s^2 \quad (9)$$

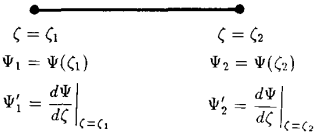

Fig. 2. Third-order Hermitian line element.

$$N_3=l(s^3-2s^2+s) \quad (10)$$

$$N_4=l(s^3-s^2) \quad (11)$$

where

$$s=\frac{\zeta-\zeta_1}{l} \quad (12)$$

$$l=\zeta_2-\zeta_1. \quad (13)$$

Using the Galerkin procedure [16] on (2), we obtain

$$-\frac{1}{\pi^2}\int_{\zeta_1}^{\zeta_2}\{N\}\frac{d}{d\zeta}\frac{1}{m^*(\zeta)}\frac{d\Psi(\zeta)}{d\zeta}d\zeta+\int_{\zeta_1}^{\zeta_2}\{N\}u(\zeta)\,\Psi(\zeta)\,d\zeta=\epsilon\int_{\zeta_1}^{\zeta_2}\{N\}\Psi(\zeta)\,d\zeta. \quad (14)$$

Integrating by parts, (14) becomes

$$\frac{1}{\pi^2}\int_{\zeta_1}^{\zeta_2}\frac{d\{N\}}{d\zeta}\frac{1}{m^*(\zeta)}\frac{d\Psi(\zeta)}{d\zeta}d\zeta-\frac{1}{\pi^2}\left[\{N\}\frac{1}{m^*(\zeta)}\frac{d\Psi(\zeta)}{d\zeta}\right]_{\zeta_1}^{\zeta_2}+\int_{\zeta_1}^{\zeta_2}\{N\}u(\zeta)\,\Psi(\zeta)\,d\zeta=\epsilon\int_{\zeta_1}^{\zeta_2}\{N\}\Psi(\zeta)\,d\zeta. \quad (15)$$

Substituting (5) into (15), for each element we obtain

$$[K]_e\{\Psi\}_e=\epsilon[M]_e\{\Psi\}_e \quad (16)$$

where

$$[K]_e=\int_{\zeta_1}^{\zeta_2}\frac{d\{N\}}{d\zeta}\frac{1}{m^*(\zeta)}\frac{d\{N\}^T}{d\zeta}d\zeta-\left[\{N\}\frac{1}{m^*(\zeta)}\frac{d\{N\}^T}{d\zeta}\right]_{\zeta_1}^{\zeta_2}+\pi^2\int_{\zeta_1}^{\zeta_2}\{N\}u(\zeta)\{N\}^T d\zeta \quad (17)$$

$$[M]_e=\pi^2\int_{\zeta_1}^{\zeta_2}\{N\}\{N\}^T d\zeta. \quad (18)$$

The second term of the right-hand side in (17) and the integration in (18) are calculated as

$$\left[\{N\}\frac{1}{m^*(\zeta)}\frac{d\{N\}^T}{d\zeta}\right]_{\zeta_1}^{\zeta_2} = \begin{bmatrix} 0 & 0 & -\dfrac{1}{m^*(\zeta_1)} & 0 \\ 0 & 0 & 0 & \dfrac{1}{m^*(\zeta_2)} \\ 0 & 0 & 0 & 0 \\ 0 & 0 & 0 & 0 \end{bmatrix} \tag{19}$$

$$\int_{\zeta_1}^{\zeta_2}\{N\}\{N\}^T d\zeta = l\begin{bmatrix} \frac{13}{35} & \frac{9}{70} & \frac{11l}{210} & -\frac{13l}{420} \\ \frac{9}{70} & \frac{13}{35} & \frac{13l}{420} & -\frac{11l}{210} \\ \frac{11l}{210} & \frac{13l}{420} & \frac{l^2}{105} & -\frac{l^2}{140} \\ -\frac{13l}{420} & -\frac{11l}{210} & -\frac{l^2}{140} & \frac{l^2}{105} \end{bmatrix} \tag{20}$$

However, the integrations in (17) must be calculated numerically because they include the functions $m^*(\zeta)$ and $u(\zeta)$.

B. Boundary Condition at the Heterointerface

Let us consider a heterointerface at $z = z_i$ of semiconductor A occupying the left ($z \leq z_i$) half space and a semiconductor B occupying the right ($z \geq z_i$) half space, as shown in Fig. 3(a). The wave functions of A and B should match smoothly with each other at the interface. However, the envelope functions Ψ_A and Ψ_B are not necessarily smooth at the interface. The boundary condition at the interface is given by

$$\begin{bmatrix} \Psi_B(z_i) \\ \nabla\Psi_B(z_i) \end{bmatrix} = T_{BA}\begin{bmatrix} \Psi_A(z_i) \\ \nabla\Psi_A(z_i) \end{bmatrix} \tag{21}$$

where $\nabla = a(d/dz)$, a is the lattice constant, and $T_{BA} = (t_{ij})$ is a 2×2 matrix called the transfer matrix [17], [18].

As shown in Fig. 3(b), let a nodal point be placed on the interface. *Element A* and *element B* denote the elements on the left-hand side and on the right-hand side of the interface, respectively, and $\Psi_{A,1}, \cdots, \Psi'_{B,2}$ denote the value of Ψ and Ψ' at each nodal point where the subscripts A, B represent the elements and 1, 2 represent the nodal points.

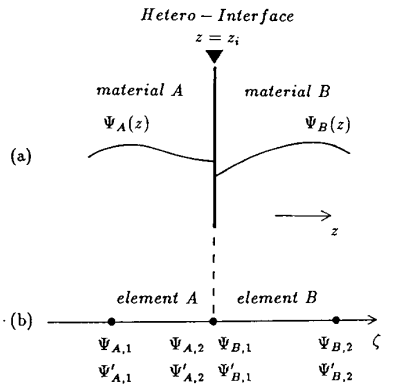

Fig. 3. Discontinuity of envelope function and definition of elements at the heterointerface.

Using $\zeta = z/d$ for (21), we obtain

$$\begin{bmatrix} \Psi_{B,1} \\ \Psi'_{B,1} \end{bmatrix} = \begin{bmatrix} t_{11} & \dfrac{a}{d}t_{12} \\ \dfrac{d}{a}t_{21} & t_{22} \end{bmatrix}\begin{bmatrix} \Psi_{A,2} \\ \Psi'_{A,2} \end{bmatrix}. \tag{22}$$

For *element B*, (16) is written as

$$[K]_e\{\Psi\}_B = \epsilon[M]_e\{\Psi\}_B \tag{23}$$

where

$$\{\Psi\}_B = [\Psi_{B,1} \quad \Psi_{B,2} \quad \Psi'_{B,1} \quad \Psi'_{B,2}]^T. \tag{24}$$

In order to eliminate $\Psi_{B,1}$ and $\Psi'_{B,1}$ from (23), we note the following relation which is derived from (22) and (24):

$$\{\Psi\}_B = [t]\{\overline{\Psi}\}_B \tag{25}$$

where

$$[t] = \begin{bmatrix} t_{11} & 0 & \dfrac{a}{d}t_{12} & 0 \\ 0 & 1 & 0 & 0 \\ \dfrac{d}{a}t_{21} & 0 & t_{22} & 0 \\ 0 & 0 & 0 & 1 \end{bmatrix} \tag{26}$$

$$\{\overline{\Psi}\}_B = [\Psi_{A,2} \quad \Psi_{B,2} \quad \Psi'_{A,2} \quad \Psi'_{B,2}]^T. \tag{27}$$

Then we obtain the following equation for *element B*:

$$[\overline{K}]_e\{\overline{\Psi}\}_B = \epsilon[\overline{M}]_e\{\overline{\Psi}\}_B \tag{28}$$

where

$$[\overline{K}]_e = [t]^T[K]_e[t] \tag{29}$$

$$[\overline{M}]_e = [t]^T[M]_e[t]. \tag{30}$$

C. Global Matrix Equation

Assembling the complete matrix for the region $\zeta_l \leq \zeta \leq \zeta_r$ by adding the contributions of all different elements, the following global matrix equation is derived:

$$[K]\{\Psi\} = \epsilon[M]\{\Psi\} \tag{31}$$

where

$$[K] = \sum_e [K]_e \tag{32}$$

$$[M] = \sum_e [M]_e. \tag{33}$$

Here the components of $\{\Psi\}$ vector are the values of Ψ and Ψ' at the nodal points in the region $\zeta_l \leq \zeta \leq \zeta_r$, and Σ_e extends over all different elements. Therefore, the order of $\{\Psi\}$ vector is $2N_p$ and the orders of $[K]$ and $[M]$ matrices are $2N_p \times 2N_p$ where N_p is the number of nodal points. $[K]_e$ and $[M]_e$ are given by (17) and (18) except for the elements on the right-hand side of the heterointerfaces. For the elements on the right-hand side of the heterointerfaces, $[\bar{K}]_e$ and $[\bar{M}]_e$ in (29) and (30) are used in place of $[K]_e$ and $[M]_e$.

By solving the generalized eigenvalue problem (31), we can obtain the eigenenergy ϵ and the value of Ψ and Ψ' at each nodal point.

Finally, it should be noted that QW's with gradual interfaces (instead of abrupt ones) can be treated within the framework of the present formalism. In this case, the transfer matrices, and therefore $[\bar{K}]_e$ and $[\bar{M}]_e$, are not necessary because Ψ and $d\Psi/d\zeta$ are continuous over all region. Potential and effective mass that vary gradually over the interfaces can be taken into account because we treat u and m^* as functions of ζ in (17) and (19).

IV. Numerical Examples

A. Rectangular Quantum Well

In order to demonstrate the validity of the present method, we first consider the eigenstates of an electron in a simple rectangular QW of GaAs/Al_xGa_{1-x}As and of InAs/GaSb, as shown in Fig. 4.

In an actual InAs/GaSb system, the top of the valence band of GaSb is higher than the bottom of the conduction band of InAs as shown in Fig. 5. Hence, the coupling between the hole in the GaSb layer and the electron in the InAs layer through the interface is important. We, however, consider the conduction band only, so that the exact solutions can be easily obtained and we can check the validity of our method.

The parameters used are given in Table I, and transfer matrices are listed below [8], [17], [19].

For GaAs/Al_xGa_{1-x}As QW,

$$T_{BA} = \begin{bmatrix} 1 & 0 \\ 0 & \dfrac{m_e^B}{m_e^A} \end{bmatrix} \tag{34}$$

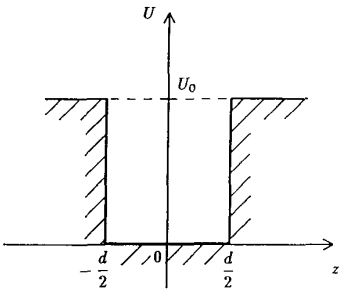

Fig. 4. Rectangular quantum well.

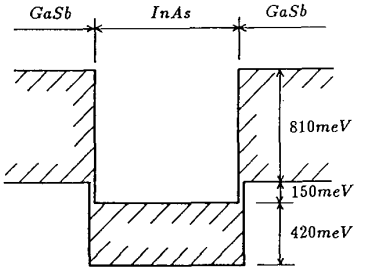

Fig. 5. Band diagram of InAs/GaSb quantum well.

TABLE I
Parameters Used in Calculation of Rectangular QW's

	$GaAs/Al_xGa_{1-x}As$ QW	$InAs/GaSb$ QW
x	0.3	—
U_0	225 meV	960 meV
d	200 Å	100 Å
m_e	$(0.067 + 0.083x)m_0$	$InAs$ $0.023m_0$ $GaSb$ $0.042m_0$
ζ_r	-3.0	
ζ_l	3.0	
N_E	92	

(m_0 : Free electron mass , N_E : Number of elements)

where m_e^A and m_e^B are the effective masses of an electron on the left- and right-hand side of the heterointerface, respectively.

For InAs/GaSb QW,

$$T_{BA} = \begin{bmatrix} -0.08 & 1.50 \\ 0.31 & -0.08 \end{bmatrix} \quad \text{(Sb: In interface)} \tag{35}$$

$$T_{BA} = \begin{bmatrix} 0.06 & 1.91 \\ 0.24 & 0.06 \end{bmatrix} \quad \text{(Ga: As interface)}. \tag{36}$$

Table II and Table III show the calculated eigenenergies of the GaAs/Al_xGa_{1-x}As QW and the InAs/GaSb QW, respectively. The results of the present method agree well with the exact solutions, not only for the well-known boundary conditions (34) (i.e., Ψ and Ψ'/m_e are continuous) at the heterointerface, but also for the general boundary conditions (35) and (36).

TABLE II
EIGENENERGIES OF $GaAs/Al_xGa_{1-x}As$ RECTANGULAR QW
$x = 0.3$, $U_0 = 225$ meV, AND $d = 200$ Å

n	Exact Solution (meV)	Finite-Element Solution (meV)
1	9.9671761	9.9671762
2	39.7718097	39.7718101
3	88.9335308	88.9335354
4	155.6079531	155.6079933

TABLE III
EIGENENERGIES OF InAs/GaSb RECTANGULAR QW
$U_0 = 960$ meV AND $d = 100$ Å

Heterojunction	n	Exact Solution (meV)	Finite-Element Solution (meV)
Ga:As As:Ga	1	74.2435974	74.2435978
	2	359.6990192	359.6990195
Sb:In In:Sb	1	89.0415776	89.0415780
	2	424.5292179	424.5292187
Ga:As In:Sb	1	83.7506551	83.7506554
	2	392.0316693	392.0316697

Figs. 6 and 7 show the well-width dependences of the eigenenergies of $GaAs/Al_{0.3}Ga_{0.7}As$ and InAs/GaSb rectangular QW's, respectively. The solid circles represent the results of our method. For comparison, we have also shown the results for the same QW's under a different, simplest, boundary condition that Ψ and Ψ' are continuous at the heterointerfaces (open circles), assuming a constant effective mass over the layers. In GaAs/AlGaAs QW, the difference between the results under the two boundary conditions is not so large. On the other hand, the difference becomes considerably large in InAs/GaSb QW. As the well width d decreases, the eigenenergy calculated with our method increases more rapidly than that of the simplest boundary condition. In particular, for the well thinner than 30 Å, there exist no bound states under the transfer-matrix boundary condition.

B. Voltage-Applied Quantum Well

Next, let us consider the QW subject to an external electric field normal to the QW layers.

In this case, there exist no bound states in an exact sense because an electron tunnels out of the well. However, if this tunneling rate is small, the states become quasi-bound and we can consider discrete energy levels [5], [7].

As described before, we consider the region $\zeta_l \leq \zeta \leq \zeta_r$, using the boundary conditions $\Psi(\zeta_l) = \Psi(\zeta_r) = 0$ at the ends of this region, which correspond to the infinite potential barriers outside this region. Therefore, when we calculate the eigenstates under this potential condition, the solutions would contain the eigenstates not only for the electron bound in the QW, but also for the electron bound

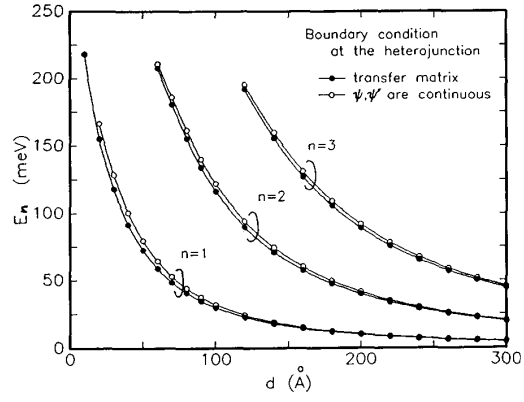

Fig. 6. Eigenenergy versus well width for $GaAs/Al_xGa_{1-x}As$ quantum well. $x = 0.3$ and $U_0 = 225$ meV.

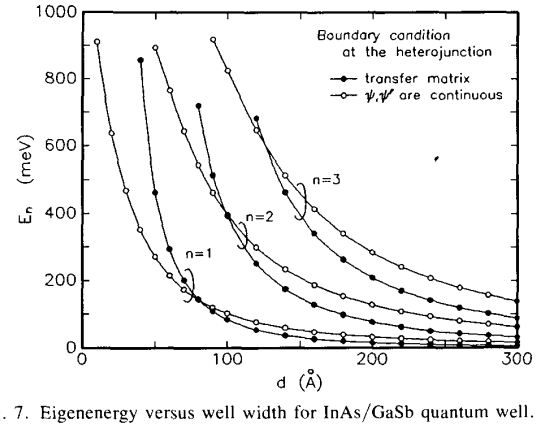

Fig. 7. Eigenenergy versus well width for InAs/GaSb quantum well. $U_0 = 960$ meV.

near the end of this region, as shown in Fig. 8. Eigenenergies and envelope functions for $m = 1$ and $m = 3$ in Fig. 8 are due to the potential condition mentioned above. These eigenstates do not exist when we consider the actual QW without such infinite potential barriers. Hence, we should discard these eigenstates to obtain correct quasi-bound states of QW. The first ($n = 1$) quasi-bound state for this QW is obtained from the eigenstate for $m = 2$ in Fig. 8. For this eigenstate, the boundary condition above is valid because the envelope function satisfies $\Psi(\zeta_l) \simeq 0$ even when the infinite potential barriers do not exist. In this way, we can obtain the quasi-bound states of the QW by selecting them out of the full solutions.

Fig. 9 shows the field dependence of energy levels in a rectangular $GaAs/Al_xGa_{1-x}As$ QW with $d = 300$ Å, $x = 0.4158$, $U_0 = 311$ meV, $N_E = 43$, $\zeta_l = -0.8$, and $\zeta_r = 0.8$. We have used the normalized unit in Fig. 9, according to Fritz [7]. Our results almost agree with his result, although he used the simplest boundary conditions. The envelope functions are also calculated for the same QW with the normalized external field $f = 0$, 10, 20, 40, and 80, as shown in Fig. 10.

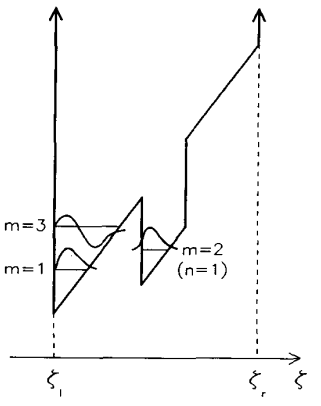

Fig. 8. Schematic diagram of eigenenergies and envelope functions of a QW subject to an external electric field under the boundary conditions $\Psi(\zeta_l) = \Psi(\zeta_r) = 0$. These boundary conditions correspond to the infinite potential barriers for $\zeta < \zeta_l$ and $\zeta > \zeta_r$. This potential profile is also shown.

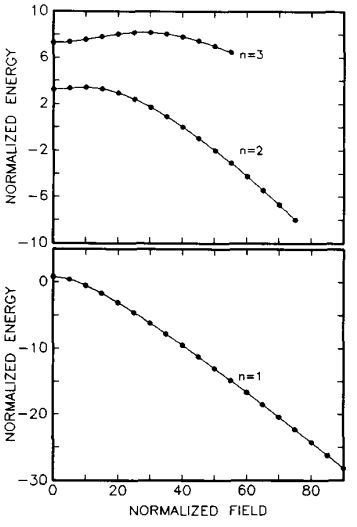

Fig. 9. Normalized eigenenergy versus normalized external electric field for $GaAs/Al_xGa_{1-x}As$ quantum well. $x = 0.3$, $U_0 = 225$ meV, and $d = 200$ Å, which correspond $u_0 = 50$ in a normalized unit.

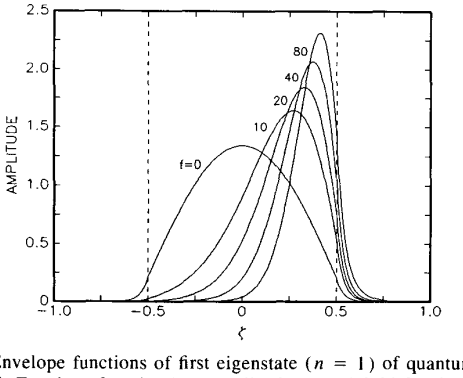

Fig. 10. Envelope functions of first eigenstate ($n = 1$) of quantum well in Fig. 8. Envelope function in normalized external field $f = 0$, 10, 20, 40, and 80 are displayed. The broken lines represent the heterointerfaces.

V. Conclusion

A finite-element method has been developed for the analysis of eigenstates in a QW which is made of arbitrary semiconductors and which has arbitrary potential profile. To take into account the general boundary condition, expressed by the transfer matrix, of the envelope function at heterointerfaces, we have used third-order Hermitian line elements. The validity of the method is confirmed by calculating the eigenstates of both GaAs/AlGaAs and InAs/GaSb QW's. The application to voltage-applied QW's also has been presented.

This approach can be extended to the calculation of transmission probability of potential barriers, which will be discussed elsewhere.

Acknowledgment

The authors would like to thank Y. Hajimoto and I. Hakamada for their continuing encouragement, and Dr. J. Nitta for helpful discussions.

References

[1] T. C. L. G. Sollner, W. D. Goodhue, P. E. Tannenwald, C. D. Parker, and D. D. Peck, "Resonant tunneling through quantum wells at frequency up to 2.5 THz," *Appl. Phys. Lett.*, vol. 43, pp. 588-590, Sept. 1983.

[2] A. R. Bonnefoi, D. H. Chow, and T. C. McGill, "Inverted base-collector tunnel transistors," *Appl. Phys. Lett.*, vol. 47, pp. 888-890, Oct. 1985.

[3] M. Yamanishi and I. Suemune, "Quantum mechanical size effect modulation light sources—A new field effect semiconductor laser or light emitting device," *Japan. J. Appl. Phys.*, vol. 22, pp. L22-L24, Jan. 1983.

[4] D. A. B. Miller, D. S. Chemla, T. C. Damen, A. C. Gossard, W. Wiegmann, T. H. Wood, and C. A. Burrus, "Electric field dependence of optical absorption near the band gap of quantum-well structures," *Phys. Rev. B*, vol. 32, pp. 1043-1060, July 1985.

[5] T. Hiroshima and R. Lang, "Well size dependence of Stark shifts for heavy-hole and light-hole levels in GaAs/AlGaAs quantum wells," *Appl. Phys. Lett.*, vol. 49, pp. 639-641, Sept. 1986.

[6] M. Matsuura and T. Kamizato, "Subbands and exitons in a quantum well in an electric field," *Phys. Rev. B*, vol. 33, pp. 8385-8389, June 1986.

[7] I. J. Fritz, "Energy levels of finite-depth quantum wells in an electric field," *J. Appl. Phys.*, vol. 61, pp. 2273-2276, Mar. 1987.

[8] Y. Ando and T. Itoh, "Calculation of transmission tunneling current across arbitrary potential barriers," *J. Appl. Phys.*, vol. 61, pp. 1497-1502, Feb. 1987.

[9] A. Harwit, J. S. Harris, Jr., and A. Kapitulnik, "Calculated quasi-eigenstates and quasi-eigenenergies of quantum well superlattices in an applied electric field," *J. Appl. Phys.*, vol. 60, pp. 3211-3213, Nov. 1986.

[10] W. W. Lui and M. Fukuma, "Exact solution of the Schrodinger equation across an arbitrary one-dimensional piecewise-linear potential barrier," *J. Appl. Phys.*, vol. 60, pp. 1555-1559, Sept. 1986.

[11] R. A. Davies, "Simulations of the current-voltage characteristics of semiconductor tunnel structures," *GEC J. Res.*, vol. 5, pp. 65-75, 1987.

[12] H. Ohnishi, T. Inata, S. Muto, N. Yokoyama, and A. Shibatomi, "Self-consistent analysis of resonant tunneling current," *Appl. Phys. Lett.*, vol. 49, pp. 1248-1250, Nov. 1986.

[13] A. N. Khondker, M. R. Khan, and A. F. M. Anwar, "Transmission line analogy of resonance tunneling phenomena: The generalized impedance concept," *J. Appl. Phys.*, vol. 63, pp. 5191-5193, May 1988.

[14] T. Miyoshi, H. Kimura, and M. Ogawa, "Electric field dependence of eigenstates in quantum wells with arbitrary potential distribution," *Trans. IEICE*, vol. E70, pp. 297-299, Apr. 1987.

[15] K. Hayata, M. Koshiba, K. Nakamura, and A. Shimizu, "Eigenstate calculation of quantum well structures using finite elements," *Electron. Lett.*, vol. 24, pp. 614–616, May 1988.
[16] O. C. Zienkiewicz, *The Finite Element Method*, 3rd ed. New York: McGraw-Hill, 1977.
[17] T. Ando and S. Mori, "Effective-mass theory of semiconductor heterojunctions and superlattices," *Surf. Sci.*, vol. 113, pp. 124–130, 1982. (The value of the transfer matrix for the InAs/GaSb heterointerface in this reference is corrected by Prof. Ando afterwards. In this paper, the value reported in the following reference is used: *Phys. Soc. Japan*, Ed., *Physics and Device Application of Semiconductor Superlattice*. Baifukan, 1984, Sect. 2 [in Japanese].)
[18] S. Mori, "A theoretical study on the electronic structures of semiconductor heterojunctions and superlattices," Doctoral dissertation, Univ. Tokyo, Japan, Dec. 1980.
[19] S. R. White and L. J. Sham, "Electronic properties of flat-band semiconductor heterostructures," *Phys. Rev. Lett.*, vol. 47, pp. 879–882, Sept. 1981.

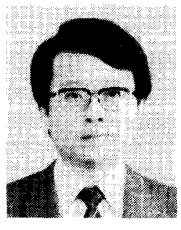

Kenji Nakamura was born in Kobe, Japan, on December 7, 1953. He received the B.S. degree in applied physics from the University of Tokyo, Tokyo, Japan, in 1978.

From 1978 to 1984 he was with the Japan Radio Company, Mitaka, Japan. In 1984 he joined the Canon Research Center, Atsugi, Japan, and is currently a Senior Engineer. He has been engaged in the research and development of surface acoustic wave devices, acoustooptic devices, laser diodes, and quantum-well physics.

Mr. Nakamura is a member of the Institute of Electronics, Information and Communication Engineers (IEICE) and the Acoustical Society of Japan.

Akira Shimizu was born in Nagano-City, Japan, on July 4, 1956. He received the B.S., M.S., and Ph.D. degrees in physics from the University of Tokyo, Tokyo, Japan, in 1979, 1981, and 1984, respectively, where he was engaged in research on superconductivity and the quantum many-body theory of random systems.

In 1984 he joined Canon Research Center, Atsugi-City, Japan, and he has been working on laser diodes, ferroelectric films, and quantum-well physics. His current major interest is optical nonlinearity of low-dimensional quantum systems and its applications.

Dr. Shimizu is a member of the Physical Society of Japan and the Japan Society of Applied Physics.

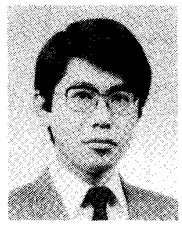

Wasanori Koshiba (SM'84) was born in Sapporo, Japan, on November 23, 1948. He received the B.S., M.S., and Ph.D. degrees in electronic engineering from Hokkaido University, Sapporo, Japan, in 1971, 1973, and 1976, respectively.

In 1976, he joined the Department of Electronic Engineering, Kitami Institute of Technology, Kitami, Japan. From 1979 to 1987, he was an Associate Professor of Electronic Engineering at Hokkaido University, and in 1987 he became a Professor. He has been engaged in research on lightwave technology, surface acoustic waves, magnetostatic waves, microwave field theory, and applications of finite-element and boundary-element methods to field problems.

Dr. Koshiba is a member of the Institute of Electronics, Information and Communication Engineers (IEICE), the Institute of Television Engineers of Japan, the Institute of Electrical Engineers of Japan, the Japan Society for Simulation Technology, and the Japan Society for Computational Methods in Engineering. In 1987, he was awarded the 1986 Paper Award by the IEICE.

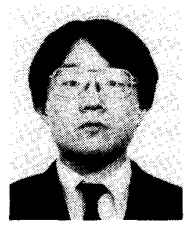

Kazuya Hayata was born in Kushiro, Japan, on December 1, 1959. He received the B.S. and M.S. degrees in electronic engineering from Hokkaido University, Sapporo, Japan, in 1982 and 1984, respectively.

Since 1984, he has been an Instructor of Electronic Engineering at Hokkaido University. His research areas have included guided-wave optics, microwave theory and techniques, surface acoustic wave (SAW) propagation, and numerical methods for field analyses. His current research activities concern nonlinear guided-wave phenomena, numerical simulation and analysis in guided-wave optics and optoelectronics, and quantum size effects in low-dimensional electron confinement structures.

Mr. Hayata is a member of the Institute of Electronics, Information and Communication Engineers (IEICE), the Japan Society of Applied Physics (JSAP), the JSAP Optics Division, and the Optical Society of America. In 1987, he was awarded the 1986 Excellent Paper Award by the IEICE.